Journal of the Chinese Society of Mechanical Engineers, Vol.47, No.1, pp75~83 (2026)

Fabrication of 3D Printed Continuous Fibre Reinforced Polymer Composites via Fused Deposition Modelling: Experimental Analysis

Narendra Kumar Jha**and Santosh Kumar*

Keywords: Continuous fiber reinforced composites, 3D printing, mechanical properties, reinforcement patterns.

ABSTRACT

Continuous fibre reinforced polymer composites are gaining attention in various industries for their ability to create complex geometries and reduce material usage through 3D printing. The previous work focused on either short or continuous fibers individually when examining the role of fiber length in stress transfer mechanisms. This study addresses the gap by investigating the integration of chopped long carbon fibers (0.1 to 1 mm) mixed with nylon as the matrix, and varying continuous fibers as reinforcements to evaluate their impact on the mechanical, thermal, and morphological properties. The experiments are performed on laminates with fiber angles [0°, 45°, 90°, 135°], varying build plate orientations [0° and 90°], and concentric reinforcement patterns. Results indicated that low temperatures improved transverse elastic modulus, strength, and in-plane shear properties, while high temperatures reduced all mechanical characteristics. Kevlar fibre reinforced composite exhibited the highest tensile strength, High strength high temperature glass fibre reinforced composite decreased by 14.66%, and flexural strength peaked at 86.22 MPa with concentric zero-degree fill.

INTRODUCTION

The lightweight engineering of aeroplanes and vehicles has recently focused heavily on thermoplastic polymers and composites. Among the several 3D printing methods that have been created, fused deposition modelling (FDM) has become the most used 3D printing methodology (Parandoush and Lin 2017) because of its low price and the broad availability of components. Short fibre-reinforced thermoplastics (SFRTs) and continuous fibre-reinforced thermoplastics (CFRTs) are the two basic groups into which they may be separated (Heidari-Rarani, Rafiee-Afarani, and Zahedi 2019). Multiple attempts have been made to look into printing parameters (Peng et al. 2020), the porous effect (Tekinalp et al. 2014), the influence of fibre orientation (Compton and Lewis 2014), and the impact of fibre content (Sodeifian, Ghaseminejad, and Yousefi 2019). For instance, (Wang et al. 2020) used the FDM printing technique to create composites made of carbon fibre (CF), glass fibre (GF), and polyetheretherketone (PEEK), as well as evaluate their mechanical characteristics. They discovered that the tensile and flexural strength were greatly enhanced with the right fibre addition, but ductility was sacrificed (Peng et al. 2021). The tensile mechanical characteristics increase initially, then decline, and then increase as the fibre content rises (Khoathane, Vorster, and Sadiku 2008; Ku et al. 2011). Therefore, modifying fibre length, content, and orientation may enhance the SFRT composite's mechanical characteristics. Researchers investigated the effects of penetration depth, extruded breadth, printing temperatures, and velocity on the tensile mechanical behavior of consistently 3D-printed carbon fiber reinf-forced polylactic acid CF-PLA composites (Dou et al. 2020). They concluded that the transmission of external loads to the carbon fibres via the fibre-matrix contact is the mechanism that strengthens the tensile mechanical characteristics. The impact of fibre orientation, however, was not studied. Numerous research studies have attempted to create CFRTs based on polyamide (PA) to enhance the qualities of FDM printing composites. The shape of the specimen significantly impacts the outcomes of the experiment. Additionally, studies on the bending features and delamination traits of CFRTs have been conducted (He et al. 2020). The findings demonstrated a substantial improvement in fracture toughness and fracture energy compared to neat PLA, particularly in composites with 0°/90° and 45°/-45° bead orientations (Papon and Haque 2019). An enhancement in tensile modulus and shear modulus was observed in the neat PLA polymer with a 15 wt% CF content in both the

Paper Received December 2024. Revised April 2025. Accepted May, 2025. Author for Correspondence: Narendra Kumar Jha.

** *Assistant Professor, Department of Mechanical Engineering, Gautam Buddha University, Greater Noida 201312, Uttar Pradesh, India*

* *Professor, Department of Mechanical Engineering, Indian Institute of Technology (BHU), Varanasi 221005, India.*

printing and transverse directions. However, the limited CF length (60 mm) restricted further mechanical improvements in the composites (Ferreira et al. 2017). In composite materials, fibers with a critical length are preferred to ensure efficient stress transfer from the matrix to the reinforcement, primarily through the shear transfer mechanism, thereby enhancing the overall load-bearing capacity of the material (Hu et al. 2020).

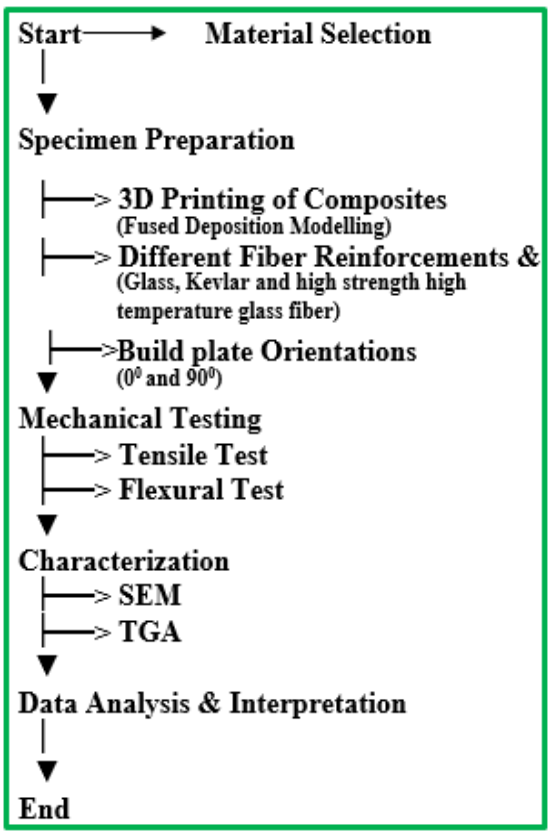

Figure 1. Flowchart of the overall experimental process of this study.

While previous studies have explored the role of fiber length in stress transfer mechanisms, they primarily focus on either short or continuous fibers individually. Short fibers are known to hinder effective stress transfer and introduce stress concentrations due to an increased number of fiber ends at the same fiber content (Arao et al. 2013). However, to the best of our knowledge, no studies have investigated the infusion of chopped long carbon fibers (0.1–1 mm) mixed with nylon as the matrix, along with (a) various continuous fiber reinforcements and (b) different build plate orientations for the development of 3D-printed continuous fiber reinforced polymer (C-FRP) composites. The novelty of this work lies in the fabrication of 3D-printed continuous fiber reinforced polymer (C-FRP) composites by integrating chopped long carbon fibers (0.1 to 1 mm) mixed with nylon as the matrix alongside varying continuous fiber reinforcements. Unlike previous studies that focus separately on either short or continuous fibers, this research uniquely explores their combined effect on the mechanical, thermal, and morphological properties of additively manufactured composites. Additionally, fused deposition modelling (FDM) is utilized to produce multiple types of continuous fiber-reinforced composite specimens, including tensile and bending specimens, allowing for a comprehensive analysis of tensile and flexural properties. The study also investigates failure behavior using scanning electron microscopy (SEM), evaluating strain fields, bonding strength, physical defects, and failure mecha nisms. Examining the effects of fiber filament fill patterns and specimen shapes on composite performance, providing critical insights into how fill patterns influence strength, modulus, and failure mechanisms. These findings contribute to the optimization of fiber reinforced additive manufacturing for improved structural applications. Results revealed that at low temperatures, transverse elastic modulus and strength, along with in-plane shear properties, improved, whereas high temperatures reduced all mechanical characteristics. These findings emphasize the role of filling patterns and reinforcements in optimizing composite designs. The overall experimental procedure adopted in this study is shown in Figure 1.

METHODOLOGY

Raw materials and 3D printing

A Markforged X7 printer as shown in Figure 2, is used to create the specimens it has an accuracy of 10 μm and is an industrial-grade printer. A 0.4 mm diameter nozzle is used to extrude nylon filament during the first stage of the C-CFRP composites printing process, and a 0.9 mm diameter nozzle is used to extrude continuous fibre filament. Through the printing nozzle, the filament can be melted into a tape with a width and thickness of around 1 mm and 0.125 mm, respectively. A nylon layer is applied to the bottom of the specimens to facilitate the deposition of C-CFRP layers onto the print bed and prevent disintegration during printing. A nylon layer was added to the top to maintain symmetmetry. The material was chosen from a 1.75 mm diameter Markforged nylon filament that was transparent in black for easy inspection. Print a layer of nylon floor first, followed by layers of continuous fibre, and then a layer of nylon roofing. Markforged Eiger software was used to develop the sample slicing strategy and fibre orientation. It is obvious that the printer of fers superb finishing. This gives the user little control over the orientations and distributions of the fibres, which might reduce the component's stiffness, partic ularly for very complicated geometries. The material was printed using onyx, and it is reinforced with glass fibre, high-strength, high-temperature fibre, and kevlar fibre. The composite typically extrudes at temperatures around 270°C, with a deposition layer height of 0.125 mm. Each test has been conducted three times under identical conditions to check the authenticity of the results. The fabricated samples are: continuous kevlar fibre polymer *(C*-KFRP) composites concentric

fibre angle zero degrees build plate orientation; continuous high strength high temperature fibre polymer (C-HSHT-GFRP) composites concentric fibre angle zero degrees build plate orientation; continuous glass fibre reinforced polymer *(C*-GFRP*)* composites concentric fibre angle zero degree build plate orientation. The thickness of each layer is 0.1 mm, and there are 24 layers. The 3D-printed composites were fabricated with a volume fraction of 17.98%.

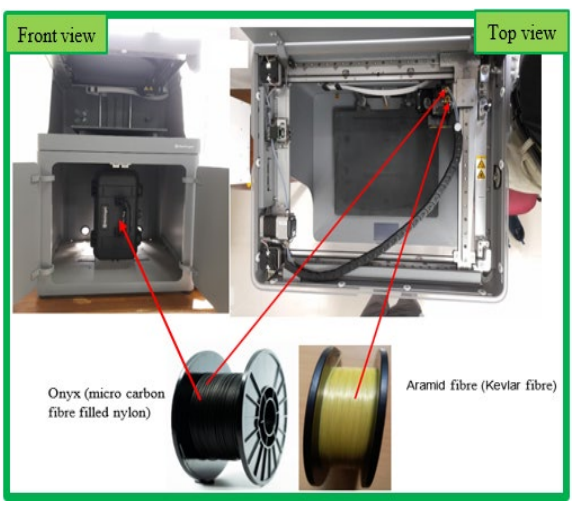

Figure 2. Schematic for the fabrication of 3D-printed continuous fiber reinforced polymer (C-FRP) composites with varying fiber reinforcements and build plate orientation.

Density of composites by displacement method

The density of a plastic specimen are determined by Archimedes principle as per ASTM D792 standards (Câmara et al. 2012).

Table 1. The measured density of 3D printed C-FRP composites with varying reinforcements.

Serial no	Composite Type	Density (g/cm^3)
1	C-GFRP (0^0)	1.2691
2	C-HSHT-GFRP(0^0)	1.2412
3	C-KFRP (0^0)	1.1214

Thermal Stability of 3D printed composites

The thermal gradient analysis (TGA) method was used to assess 3D printed composites thermal stability, degradation characteristics, and adsorption quality. Fibers remain stable without decomposing up to 800°C, whereas nylon starts thermal decomposition at 260°C.

Figure 3 presents the TGA test results for the (a) 3D-printed C-KFRP (0°) and C-HSHT-GFRP (0°) composites (Saeed et al. 2021). After the complete decomposition of nylon, the remaining mass represents the fibers. At temperatures between 100°C and 350°C, a modest decrease in weight is noted, most likely as a result of water evaporation. The mass of the nylon component in the composites decreased as a result of decomposition at 350°C, and full decomposition happens at 500°C. TGA analysis of 3D-printed C-FRP composites with varying reinforcements revealed that fiber mass fraction remained unaffected by the reinforcement type. Both C-HSHT-GFRP (0^0) and C-GFRP (0^0) composites exhibit similar degradative behaviour. The C-HSHT-GFRP (0°) composite samples demonstrate excellent thermal stability, as indicated by a weight loss of only 6% for C-HSHT-GFRP (0°) and 9% for C-KFRP (0°) when heated from room temperature to 400°C. The higher residue at 900°C—29% for C-HSHT-GFRP (0°) compared to 19% for C-KFRP (0°) further supports the superior thermal stability of the C-HSHT-GFRP (0°) composite. Additionally, the specific surface area calculated from the TGA plot reveals that the C-KFRP (0°) composite has the highest surface area, indicating its greater adsorptive capacity compared to C-HSHT-GFRP (0°) and C-GFRP (0°) composites. This higher surface area suggests that C-KFRP (0°) may interact more effectively with surrounding materials or gases, contributing to its unique properties.

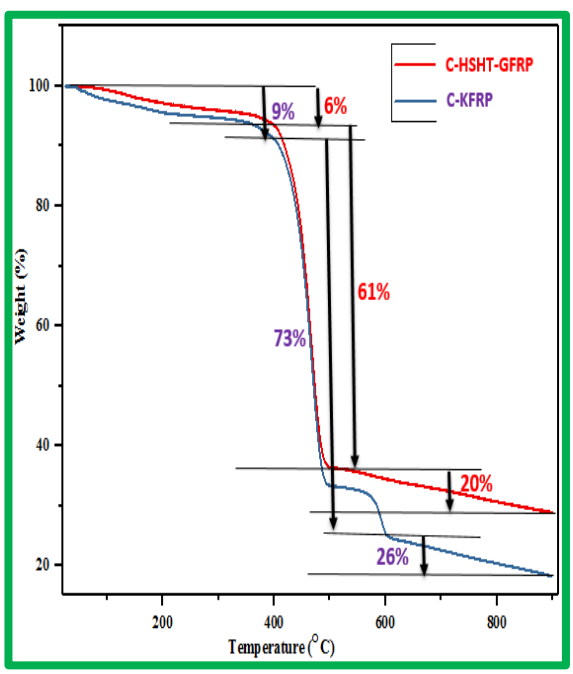

Figure 3. TGA curves illustrating the thermal degradation behavior of 3D-printed C-KFRP (0°) and C-HSHT-GFRP (0°) composites.

Table 2. Measurement of specific surface area of 3D printed C-FRP composites with varying reinforcements.

Serial number	Composite	Specific surface area (cm^2/g)
1	C-HSHT-GFRP (0^0)	5.73
2	C-KFRP (0^0)	7.29
3	C-GFRP (0^0)	7.12

RESULTS AND DISCUSSION

Mechanical properties

Tensile properties. Tensile tests are performed in accordance with the ASTM D638 standard, as illustrated in Figure 4.

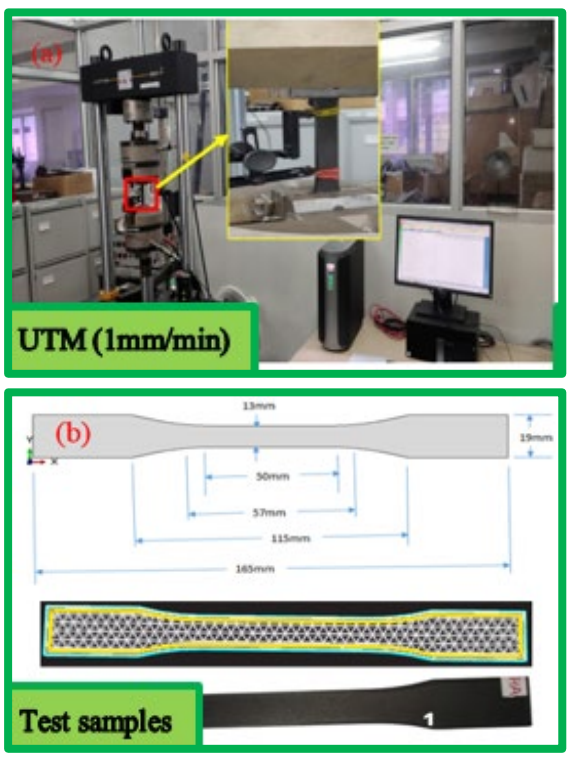

Figure 4. Experimental setup for assessing the mechanical properties such as tensile strength and modulus etc of 3D-printed C-FRP composites.

The results of tensile tests for nylon, onyx and 3D printed C-FRP composites with varying reinforcements and build plate orientations were given in Figure 5, Figure 6 and Table 3. Compared to the neat onyx matrix, C-KFRP composites had the largest tensile strength with an enhancement of 208% from 40MPa to 124MPa with the addition of kevlar fiber reinforce ments. This 208% increase suggests that kevlar fibers play a crucial role in reinforcing the polymer matrix, likely due to their high strength-to-weight ratio and excellent energy absorption properties. Kevlar fibers are well known for their toughness and resistance to impact and tensile loads, which explains their effect tiveness in enhancing the composite's mechanical properties. Furthermore, the variations in reinforce ment types and build plate orientations in the 3D printing process could influence the overall performance of the composites. The fiber alignment, layer adhesion, and fiber-matrix interaction are critical factors that determine the final strength of the printed material. The substantial improvement in tensile strength suggests that the fiber-matrix bonding in C-KFRP composites is effective, allowing for efficient stress transfer between the matrix and the reinforcement. In comparison to nylon and pure onyx, it is likely that all fiber-reinforced composites demonstrate superior tensile performance, with kevlar reinforcement standing out as the most effective. Future studies could further explore plore how different fiber volume fractions, orientations, and hybrid reinforcements impact the tensile properties of these 3D-printed composites (Tekinalp et al. 2014; Sodeifian, Ghaseminejad, and Yousefi 2019).

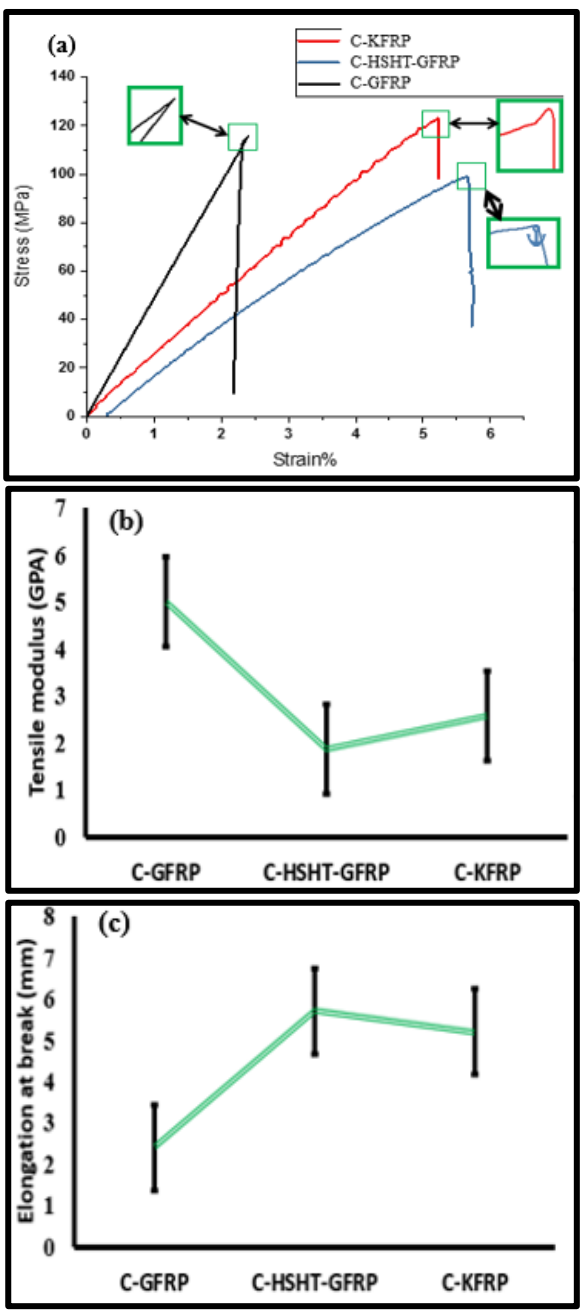

Figure 5. Tensile properties of 3D printed C-FRP composites with varying reinforcements: (a) tensile strength, (b) tensile modulus and (c) elongation at break .

Figure 5 shows that stress and strain both rise as concentric fibre rings and fibre layers increase (Wang et al. 2020). While the nylon matrix remained intact, the

fibers within the specimen fractured. Being a polymer, nylon exhibits greater elasticity. However, when the number of concentric fibre rings and layers increases, the specimen breaks abruptly and clearly exhibits brittleness. The C-KFRP composite shows the maximum tensile strength of 124 MPa, followed by C-GFRP having a tensile strength of 116 MPa, and the C-HSHT-GFRP composite shows the least value of tensile strength of 99 MPa. A similar type of explanations are also reported elsewhere (Peng et al. 2020); it is due to the difference in the strength of individual fibres where the kevlar has a strength of 610 Mpa followed by C-HSHT-GFRP of 600 MPa fibre glass, is having the least value of 590 MPa (Parandoush and Lin 2017). The key point is that the strength difference between each successive fiber is only 10 MPa, whereas these differences become more pronounced in the final fabricated composites. The tensile strength of continuous GFRP is 116 MPa, which is greater than the value found in ref. (Heidari-Rarani, Rafiee-Afarani, and Zahedi 2019). The order of tensile strength is C-KFRP > C-GFRP > C-HSHT-GFRP composites. The longitudinal tensile failure strain of 3D printed C-HSHT-GFRP composites is approximately 5.65%, and it is the highest value of failure strain compared with the other two composites. The longitudinal tensile failure strain of C-KFRP composites is 5.22%. The longitudinal tensile failure strain of C-GFRP composites is 2.4%. Therefore, from the stress-strain curve, it is found that C-GFRP composites show the most brittle behavior. Moreover, the nature of the curve is also the confirmation of the brittle behavior of the material. The C-GFRP composites have a sharp yield point compared to the other two composites, which is easily visible in an enlarged view. The order of sharpness in the yield point is as follows: C-GFRP > C-KFRP > C-HSHT-GFRP composites. As the ductility of a material decreases, the value of stiffness increases (Tian et al. 2017; Dickson et al. 2017). Elastic modulus is listed in the following sequence: C-GFRP > C-KFRP > C-HSHT-GFRP Composites.

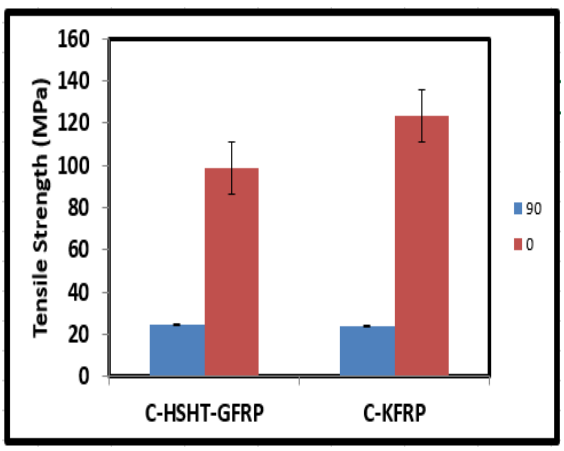

Figure 6. Tensile strength of 3D printed C-FRP composites with varying build plate orientations.

Table 3. Mechanical properties of nylon, onyx and 3D printed C-FRP composites with varying reinforcements and build plate orientations.

Samples	Tensile strength (MPa)	Tensile modulus (GPa)	Elongation at break (mm)	Flexural strength (MPa)	Flexural modulus (GPa)
Nylon	51	1.7	1.5	50	1.4
Onyx	40	2.4	0.25	71	3
C-GFRP	$116(0^0)$	5	2.4	86	4
C-HSHT-GFRP	$99(0^0)$, $25(90^0)$	1.86	5.7	$50(0^0)$, $84(90^0)$	1.3
C-KFRP	$124(0^0)$, $24(90^0)$	2.58	5.2	$46(0^0)$, $79(90^0)$	1.25

Three-point bending properties

Assessing the flexural properties of composites is essential to prevent deflection and bending fractures under high loads and sliding velocities in certain engineering applications. With this in mind, flexural tests were performed using the three-point bending method to compare neat nylon, onyx and 3D printed C-FRP composites with varying reinforcements and build plate orientations. The specimens were prepared as per ASTM D 790 standard, as illustrated in Figure 7 and the Flexural properties of 3D printed C-FRP composites with varying reinforcements and build plate orientation is shown in Figure 8. The flexural test results highlight the influence of fiber type and infill orientation on the mechanical performance of 3D-printed composites. The C-GFRP composites demonstrate a significant improvement in both flexural strength (98 MPa, +43%) and modulus (4 GPa, +33%) compared to the neat onyx matrix when using a concentric zero-degree filling pattern. This suggests that glass fibers effectively enhance the load-bearing capacity and stiffness of the composite under bending loads. Influence of fiber Type: Interestingly, despite kevlar's high tensile strength, the kevlar-reinforced composite exhibits a 35% reduction in flexural strength compared to neat Onyx. This may be attributed to kevlar's relatively lower compressive strength compared to glass fiber. In flexural testing, the material undergoes both tension and compression, kevlar's superior tensile properties help in tension but its lower compressive strength likely reduces the overall flexural performance. Effect of Infill orientation.

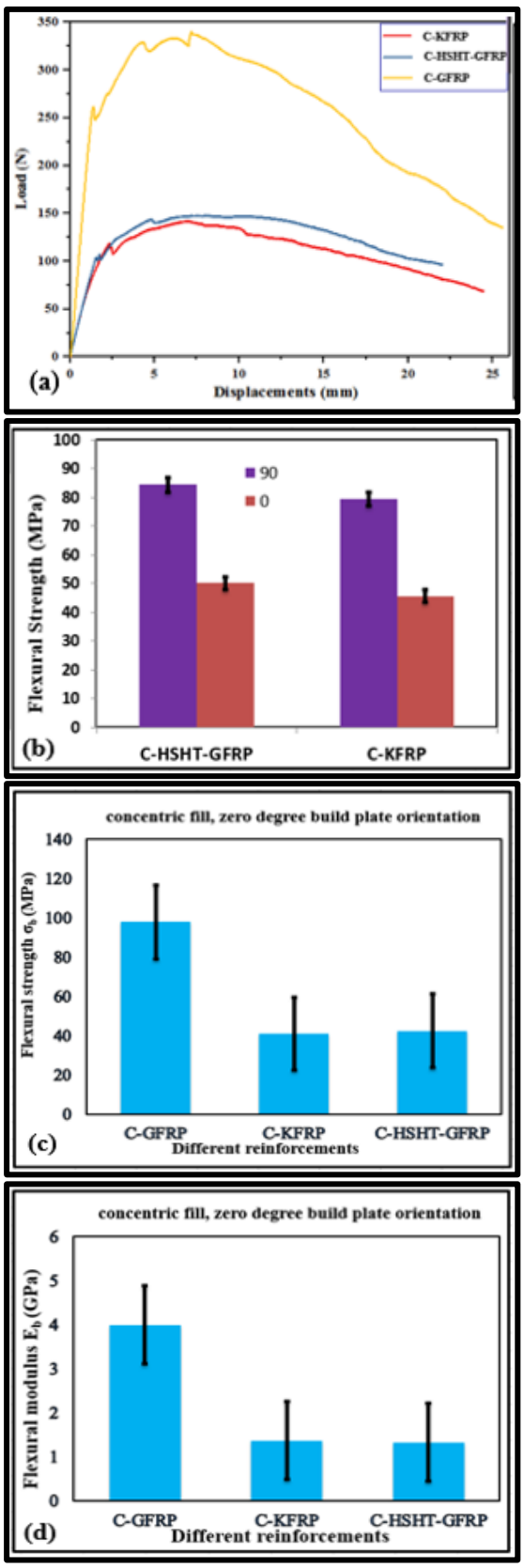

Figure 7. Experimental setup for assessing the Flexural properties of 3D-printed C-FRP composites of different reinforcements and build plate orientation.

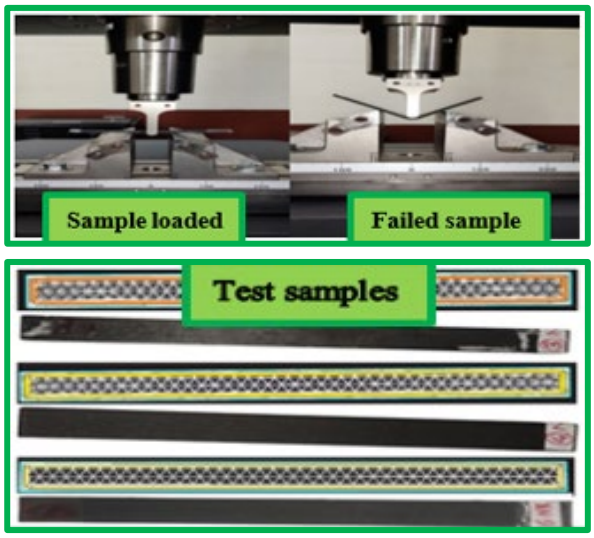

Figure 8. Flexural properties of 3D printed C-FRP composites with varying reinforcements: (a) Load-displacement curve, (c) flexural strength and (d) flexural modulus (b) flexural strength with varying build plate orientation.

The study also reveals that the concentric 90-degree infill pattern out performs the zero-degree pattern in flexural performance. This is likely due to better load distribution and fiber alignment perpendicular to the loading direction, which enhances resistance to bending stresses. In contrast, the zero-degree pattern may align fibers in a way that does not effectively counteract bending forces, making the material more susceptible to failure. Stiffness Performance: Among the tested configurations, the glass fiber composite with a zero-degree concentric infill pattern exhibits the highest stiffness. This indicates that glass fibers provide superior resistance to deformation under bending loads, making them ideal for applications requiring high rigidity. These findings emphasize the importance of fiber selection and print orientation in optimizing 3D-printed composite performance. While kevlar fibers are beneficial for tensile strength, glass fibers appear more effective in improving flexural properties. Additionally, adjusting the infill pattern can significantly influence the mechanical behavior, with a 90-degree concentric infill proving superior in flexural resistance. The failure mechanisms observed under bending strain in 3D-printed fiber-reinforced composites reveal a complex interplay between the fibers and the matrix. The fracture surface is divided into two distinct regions: the upper compressive zone experiences compression failure in the fibers and matrix fracture. The fibers undergo buckling and crushing, while the matrix, which is more brittle, fails due to compressive stress. The Lower Tensile region is dominated by fiber tensile failure, fiber pull-out, and matrix fracture. The fibers play a critical role in bearing the tensile load, and their failure often leads to a catastrophic breakdown of the composite. Fiber pull-out occurs when the bonding between the fiber and

matrix is weak, leading to a reduction in load transfer efficiency. The order of bending properties is as follows: C-GFRP > C-KFRP > C-HSHT-GFRP Composites.

FRACTOGRAPHY AND FAILURE ANALYSIS

The fracture surfaces of the various fibre-reinforced composites were investigated using a scanning electron microscope (SEM) to determine the fibre pull-out behaviour from the matrix. This depicts the bonding of the fibre and matrix interface; it is clear from the diagram that several types of failure occurred following destructive testing. The different types of failure are cohesive failure, adhesive failure, matrix debonding, and fibre pulled out, as can be observed in Figure 9.

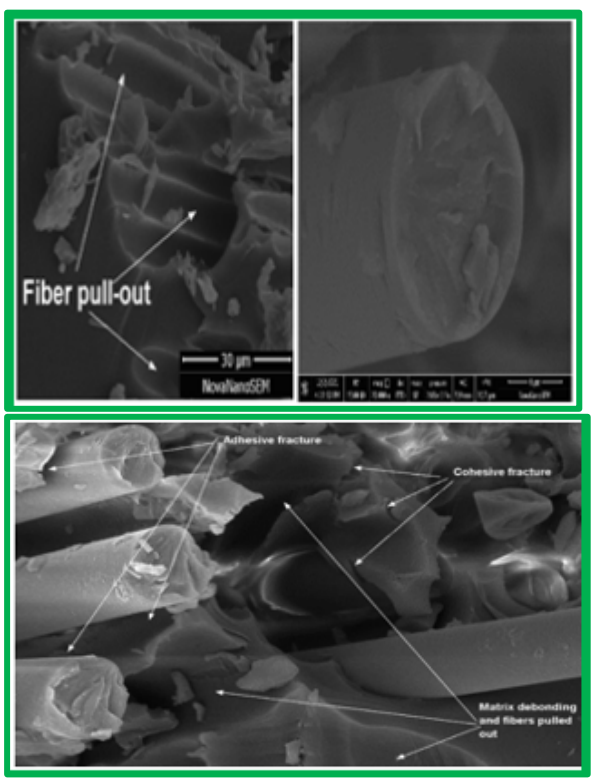

Figure 9. SEM images depicting fracture morphology of 3D-printed C-FRP composites with different reinforcements after tensile failure.

The pull-out behaviour of glass fibre is demonstrated when the fibre separates material depositions that were observed imply a somewhat excellent interface connection between the fibre and matrix, which means that a small amount of fibre from the matrix material slips off during the tensile test. The fibre pull-out from the matrix material has a smooth surface with very little matrix material deposition on the Surface of the fibre. This smooth surface is an indication of poor fibre and matrix interface bonding. The creation and spread of cracks are readily apparent and result in failure. Figure 10 shows the fibre pull-out behaviour of HSHT glass fibre. The fibre pulls away from the matrix material. It shows extra matrix material deposition on the surface of the fibre. The observed more matrix material deposition on the fibre's surface suggests a strong interface bonding of the fibre and matrix and implies nearly no slippage of fibre from the matrix, consistent with prior research published (Dickson et al. 2017). The HSHT glass fibre reinforced 3D printed polymer composite is stiffer due to the strong interface bonding, which causes brittle fracture. As a result, it is clear from Figure 10 that when compared to specimens reinforced with glass and kevlar fibres, HSHT glass fibre reinforced 3D printed polymer composite specimens had the strongest interface bonding. The figure illustrates how fibre pull-out impressions are more common than fracture impressions. Additionally, the fibres and matrix have been substantially deformed by the collision. Based on the fracture surface analysis, it seems like the material is flowing slowly. According to mor-phological studies, the main reason composites fail is fibre breakage, which results from the composite's brittle nature.

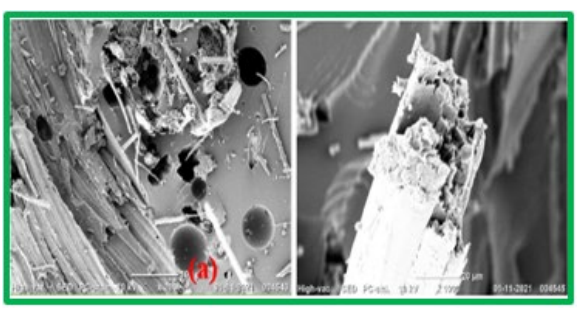

Figure 10. SEM images depicting fracture morphology of 3D-printed C-FRP composites with different reinforcements after (a) bending fracture surface and fibre pull out.

CONCLUSION

In this work, the infusion of chopped long cabon fibers (0.1–1 mm) mixed with nylon to form the matrix, along with (a) various continuous fiber reinforcements and (b) different build plate orientations, was utilized for the development of 3D-printed continuous fiber reinforced polymer (C-FRP) composites using FDM-based printing. To study the mechanical properties of these 3D-printed C-FRP composites, tensile tests, flexural tests, TGA, and SEM characterization techniques were employed. The TGA analysis of 3D-printed composites shows that fibers remain stable up to 800°C, while nylon decomposes at 260°C, fully degrading by 500°C. Both C-HSHT-GFRP (0°) and C-GFRP (0°) exhibit similar degradation, but C-HSHT-GFRP (0°) shows superior thermal stability with only 6% weight loss at 400°C and 29% residue at 900°C. C-KFRP (0°) has the highest specific surface area, indicating greater adsorption capacity. These findings suggest C-HSHT-GFRP (0°) is ideal for high-temper-

ature applications, while C-KFRP (0°) excels in adsorption-based applications, offering diverse utility based on thermal and surface interaction needs.

The tensile analysis of 3D-printed C-FRP composites demonstrates a significant enhancement in mechanical properties with fiber reinforcement. Among the tested materials, C-KFRP composites exhibit the highest tensile strength of (124 MPa, +208%) followed by C-GFRP at 116 MPa and C-HSHT-GFRP at 99 MPa, highlighting the superior reinforcing effect of kevlar fibers due to their high strength-to-weight ratio and energy absorption capabilities. The differences in fiber strength become more pronounced in the final fabricated composites, emphasizing the role of fiber-matrix bonding and alignment in determining tensile performance. The failure strain analysis reveals that C-HSHT-GFRP composites have the highest failure strain at 5.65%, indicating greater ductility, whereas C-GFRP composites display the most brittle behavior with a sharp yield point. The order of tensile strength and stiffness follows the trend: C-KFRP > C-GFRP > C-HSHT-GFRP, confirming that kevlar reinforcement provides the greatest mechanical improvement. These findings suggest that fiber selection, volume fraction, and orientation play a crucial role in optimizing the tensile performance of 3D-printed composites for various applications.

The flexural test results highlight the critical role of fiber type and infill orientation in determining the mechanical performance of 3D-printed fiber-reinforced composites. Glass fiber reinforced composites (C-GFRP) exhibited the highest flexural strength (98 MPa, +43%) and modulus (4 GPa, +33%) compared to the neat onyx matrix, demonstrating their superior load-bearing and stiffness properties. Despite kevlar's high tensile strength, its reinforcement resulted in a 35% reduction in flexural strength due to its lower compressive strength, highlighting the limitations of kevlar in bending applications. The study also revealed that a 90-degree concentric infill pattern enhances flexural resistance more effectively than a 0-degree pattern, likely due to improved load distribution and fiber alignment. Additionally, failure analysis indicated distinct fracture mechanisms, with compression failure occurring in the upper region and fiber tensile failure dominating the lower tensile zone. The findings emphasize that glass fibers are more effective in enhancing flexural properties, while infill orientation significantly impacts bending resistance. The overall order of flexural performance is C-GFRP > C-KFRP > C-HSHT-GFRP composites, reinforcing the need for tailored fiber selection and printing strategies for optimizing mechanical behavior in 3D-printed composites. SEM analysis confirmed stronger fiber-matrix interface bonding in HSHT glass fiber-reinforced composites, leading to a more brittle fracture, while kevlar-reinforced composites exhibited smoother fiber pull-out surfaces, indicating weaker bonding and higher energy absorption potential.

Future scope: future research can explore optimizing fiber volume fractions, orientations, and hybrid reinforcements to enhance thermal and mechanical properties of 3D-printed composites. Computational modelling and AI-driven design can optimize material properties for aerospace, automotive, and structural industries applications.

REFERENCES

Arao, Yoshihiko, S Yumitori, H Suzuki, T Tanaka, K Tanaka, and TJCPAAS Katayama. 2013. 'Mechanical properties of injection-molded carbon fiber/polypropylene composites hybridized with nanofillers', *Composites Part A: Applied Science and Manufacturing*, 55: 19-26.

Câmara, MA, JC Campos Rubio, AM Abrão, and JP Davim. 2012. 'State of the art on micromilling of materials, a review', *Journal of Materials Science & Technology*, 28: 673-85.

Compton, Brett G, and Jennifer A Lewis. 2014. '3D printing: 3d-printing of lightweight cellular composites (Adv. Mater. 34/2014)', *Advanced Materials*, 34: 6043-43.

Dickson, Andrew N, James N Barry, Kevin A McDonnell, and Denis P Dowling. 2017. 'Fabrication of continuous carbon, glass and Kevlar fibre reinforced polymer composites using additive manufacturing', *Additive Manufacturing*, 16: 146-52.

Dou, Hao, Yunyong Cheng, Wenguang Ye, Dinghua Zhang, Junjie Li, Zhoujun Miao, and Stephan Rudykh. 2020. 'Effect of process parameters on tensile mechanical properties of 3D printing continuous carbon fiber-reinforced PLA composites', *Materials*, 13: 3850.

Ferreira, Rafael Thiago Luiz, Igor Cardoso Amatte, Thiago Assis Dutra, and Daniel Bürger. 2017. 'Experimental characterization and micrography of 3D printed PLA and PLA reinforced with short carbon fibers', *Composites Part B: Engineering*, 124: 88-100.

He, Qinghao, Hongjian Wang, Kunkun Fu, and Lin Ye. 2020. '3D printed continuous CF/PA6 composites: Effect of microscopic voids on mechanical performance', *Composites science and technology*, 191: 108077.

Heidari-Rarani, Mohammad, M Rafiee-Afarani, and AM Zahedi. 2019. 'Mechanical characterization of FDM 3D printing of continuous carbon fiber reinforced PLA composites', *Composites Part B: Engineering*, 175: 107147.

Hu, Chao, Jiaqi Dong, Junjie Luo, Qing-Hua Qin, and Guangyong Sun. 2020. '3D printing of chiral carbon fiber reinforced polylactic acid

composites with negative Poisson's ratios', *Composites Part B: Engineering*, 201: 108400.

Khoathane, MC, OC Vorster, and ER Sadiku. 2008. 'Hemp fiber-reinforced 1-pentene/polypropylene copolymer: the effect of fiber loading on the mechanical and thermal characteristics of the composites', *Journal of reinforced plastics and composites*, 27: 1533-44.

Ku, Harry, Hao Wang, N Pattarachaiyakoop, and Mohan Trada. 2011. 'A review on the tensile properties of natural fiber reinforced polymer composites', *Composites Part B: Engineering*, 42: 856-73.

Papon, Easir Arafat, and Anwarul Haque. 2019. 'Fracture toughness of additively manufactured carbon fiber reinforced composites', *Additive Manufacturing*, 26: 41-52.

Parandoush, Pedram, and Dong Lin. 2017. 'A review on additive manufacturing of polymer-fiber composites', *Composite Structures*, 182: 36-53.

Peng, WANG, ZOU Bin, DING Shouling, LI Lei, and Chuanzhen Huang. 2021. 'Effects of FDM-3D printing parameters on mechanical properties and microstructure of CF/PEEK and GF/PEEK', *Chinese Journal of Aeronautics*, 34: 236-46.

Peng, Xingshuang, Miaomiao Zhang, Zhengchuan Guo, Lin Sang, and Wenbin Hou. 2020. 'Investigation of processing parameters on tensile performance for FDM-printed carbon fiber reinforced polyamide 6 composites', *Composites Communications*, 22: 100478.

Saeed, Khalid, Alistair McIlhagger, Eileen Harkin-Jones, John Kelly, and Edward Archer. 2021. 'Predication of the in-plane mechanical properties of continuous carbon fibre reinforced 3D printed polymer composites using classical laminated-plate theory', *Composite Structures*, 259: 113226.

Sodeifian, Gholamhossein, Saghar Ghaseminejad, and Ali Akbar Yousefi. 2019. 'Preparation of polypropylene/short glass fiber composite as Fused Deposition Modeling (FDM) filament', *Results in Physics*, 12: 205-22.

Tekinalp, Halil L, Vlastimil Kunc, Gregorio M Velez-Garcia, Chad E Duty, Lonnie J Love, Amit K Naskar, Craig A Blue, and Soydan Ozcan. 2014. 'Highly oriented carbon fiber–polymer composites via additive manufacturing', *Composites science and technology*, 105: 144-50.

Tian, Xiaoyong, Tengfei Liu, Qingrui Wang, Abliz Dilmurat, Dichen Li, and Gerhard Ziegmann. 2017. 'Recycling and remanufacturing of 3D printed continuous carbon fiber reinforced PLA composites', *Journal of cleaner production*, 142: 1609-18.

Wang, Peng, Bin Zou, Shouling Ding, Chuanzhen Huang, Zhenyu Shi, Yongsheng Ma, and Peng Yao. 2020. 'Preparation of short CF/GF reinforced PEEK composite filaments and their comprehensive properties evaluation for FDM-3D printing', *Composites Part B: Engineering*, 198: 108175.